

3D Descriptor for an Oriented-human Classification from Complete Point Cloud

Kyis Essmaeel, Cyrille Migniot and Albert Dipanda

LE2I-CNRS, University of Burgundy, Dijon, France

Keywords: Human Classification, Histogramm of Oriented Normals, 3D Point Cloud.

Abstract: In this paper we present a new 3D descriptor for the human classification. It is applied over a complete point cloud (i.e 360° view) acquired with a multi-kinect system. The proposed descriptor is derived from the Histogram of Oriented Gradient (HOG) descriptor : surface normal vectors are employed instead of gradients, 3D points are expressed on a cylindrical space and 3D orientation quantization are computed by projecting the normal vectors on a regular polyhedron. Our descriptor is utilized through a Support Vector Machine (SVM) classifier. The SVM classifier is trained using an original database composed of data acquired by our multi-kinect system. The evaluation of the proposed 3D descriptor over a set of candidates shows very promising results. The descriptor can efficiently discriminate human from non-human candidates and provides the frontal direction of the human with a high precision. The comparison with a well known descriptor demonstrates significant improvements of results.

1 INTRODUCTION

Human detection has been an important research subject in computer vision for many years. It is used in a wide variety of applications including health monitoring, driving assistance, video games and behavior analysis. It is particularly a challenging problem for many reasons. Pose, color and texture significantly vary from one person to another, besides the complexity of the working environment represents another challenge to overcome. While most of the approaches for human detection rely on color-image, the recent advances in depth sensor technology provided additional solutions. The introduction of affordable and reliable depth sensors like the kinect from Microsoft has dramatically increased the interest of these technologies and is leading to a huge number of applications using such sensors. Human detection was one of the first domains to use this new technology and exploit its benefits. Depth information is most of the time used to reduce the computation cost. However the descriptiveness of the 3D shape of the human envelop was never really exploited.

There are two main categories of methods for human detection: descriptor/classifier (Figure 1) and matching templates. In the first category, HOG (Histogram of Oriented Gradients) (Dalal and Triggs, 2005) is considered as one of the most successful descriptor

for 2D image human detection. It is used most of the time with SVM as a classifier. The HOD (Histogram of Oriented Depths) (Spinello and Arras, 2011; Choi et al., 2013) is a well-known adaptation of the HOG which is applied on depth images. HOD locally encodes the direction of depth changes and relies on a depth-informed scale-space search. In fact it uses the depth array as a 2D image to apply the HOG process. Hence 3D data are not exploited in their first forms, which makes them difficult to apply in scenarios where multiple sources of information are combined to produce the 3D data like in a multi-sensor system. The Relational Depth Similarity Features (RDSF) (Ikemura and Fujiyoshi, 2011) arise the same problem as before. The RDSF calculate the degrees of similarity between all of the combinations of rectangular regions inside a detection window in a single depth image only. The second category of methods rely on matching one or many templates of certain body-parts in 2D data (images) or 3D data (point clouds). The Ω -shape of the head and shoulders of a human body are an example of descriptive templates (Tian et al., 2013). To compare it to the data, Xia (Xia et al., 2011) uses chamfer distance and Choi (Choi et al., 2011) uses the Hamming distance.

In this paper we propose a human classification method that operates on point clouds and exploits uniquely the 3D features of the human without using

color information. The proposed 3D descriptor can be considered as a generalization of the HOG descriptor. The calculation of the descriptor starts by dividing the 3D cloud into 3D blocks. The 3D descriptor is then obtained by computing the histogram of orientations of the normals on the points in each block similarly to (Tang et al., 2012). Song (Song and Xiao, 2014) uses also the normals to describe 3D object. For his learning, he renders each example from different view angles. In our method we set an orientation for the learning. Hence we increase the descriptivity of our model and we can estimate the orientation of the frontal direction. Finally we use a SVM classifier to determine whether the 3D descriptor represents a human or not. Moreover, the descriptor provides additional information about the frontal orientation of the human. Such information is important for numerous applications namely tracking initialization, human-machine interaction and behavior analysis.

For optimal performance the proposed method is applied on a Complete Point Cloud (CPC). Indeed the isotropic property of the CPCs (i.e 360° view) allows the estimation of the frontal orientation contrary to other types of data. In our case we employ a multi-kinect platform to capture the CPC. Building a multi-kinect system requires dealing with several challenges like calibration, interference and noise removing (Essmaeel et al., 2012). The platform covers the entire working environment and thus the complete 3D shape of the subject is reconstructed. Exploiting 3D data

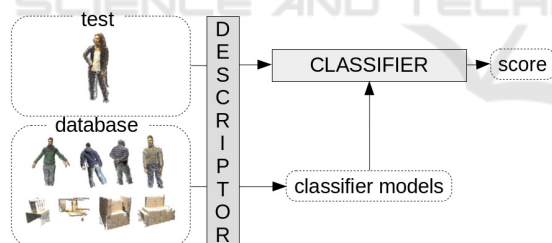


Figure 1: Overview of the descriptor/classifier framework. The descriptor transforms the data into a more descriptive space. A classifier is built from the database of positives and negatives examples. The classifier computes for each candidate a classification score.

has recently become easier after the arrival of reliable and affordable depth sensors like the kinect. In addition, the flexibility of these sensors allows building 3D acquisition systems that combine multiple units. Such 3D acquisition systems can provide now accurate and reliable measurements. These systems can be used even for high level applications like medical applications that require a complete view of persons in a controlled environment. In a complete 3D view it is guaranteed to capture more valuable information about the studied subjects. For example in a

3D model of a person the side view is less descriptive than the front view, this information can be helpful to determine the frontal direction of a person. Also In classification applications fewer training examples are required since a complete 3D training model can capture more variation of the targeted class at once. The paper is organized as follows. Section 2 presents our framework for human classification, in this we detail our acquisition system, the new descriptor we propose and the classification process. Section 3 gives the experimental results that validates our method. Comparison with single view processes is performed. Section 4 draws the conclusions.

2 HUMAN CLASSIFICATION

The proposed method for an oriented human classification follows the descriptor/classifier approach. It requires a complete 3D point cloud. A descriptor is computed from a point cloud to transfer the raw data into more descriptive information, then a classification model is built using the SVM machine learning algorithm.



Figure 2: An example of a CPC from different points of view.

2.1 Acquisition System

The 3D descriptor is computed from a CPC i.e a 360° view (Figure 2). In order to achieve this complete coverage of the scene a multi-kinect platform is constructed. The platform consists of three kinects positioned so that two consecutive kinects share an overlapping field of view. The multi-kinect system is then calibrated to obtain the extrinsic and the intrinsic parameters for each kinect.

The intrinsic parameter are required to transfer the 2D

depth image into a 3D point cloud while the extrinsic parameters allows the transformation of the point clouds from each kinect to a commune coordinate system. There are many efficient methods to compute these parameters (Deveaux et al., 2013; Raposo et al., 2013). The kinect calculates the depth image via structured light imaging technology. For this, the kinect uses an infra-red light projector to project a pattern on the scene. The kinect captures the projected pattern via its inferred camera. Then the disparity d is calculated from this pattern and a pre-registered one at known distance. The depth is then computed as the inverse of the disparity using the following equation:

$$z = \frac{1}{c_v \times d + c_u} \quad (1)$$

where c_u and c_v are the image central point coordinates.

The depth camera follows a pin-hole camera model. From this the 3D world points are projected on image plane according to the equation:

$$\begin{pmatrix} u \\ v \\ 1 \end{pmatrix} = K \times \begin{pmatrix} x \\ y \\ z \end{pmatrix} \quad \text{with } K = \begin{pmatrix} f_u & 0 & c_u \\ 0 & f_v & c_v \\ 0 & 0 & 1 \end{pmatrix} \quad (2)$$

where K is the matrix of the intrinsic parameters of the camera, f_u and f_v are the focal length. So we have:

$$x = z \frac{u - c_u}{f_u} \quad \text{and} \quad y = z \frac{v - c_v}{f_v} \quad (3)$$

The extrinsic parameters are the rotation $R_{i,o}$ and translation $T_{i,o}$ matrices between each kinect frame F_i and a reference frame F_o (which is usually overposed on one of the kinects). Hence, the point cloud pc_i captured by any kinect is transformed to the reference frame by means of its rotation and translation matrices. Finally the complete point cloud PC is obtained as follows:

$$PC = \bigcup_{i \in [1, N]} R_{i,o} \times pc_i + T_{i,o} \quad (4)$$

where N is the number of kinects in the platform. The applications that will exploit our methods take place mainly in an indoor environment that contains large planar surfaces (ground, walls). Thus a modified RANSAC algorithm (Fischler and Bolles, 1981) is applied to the acquired CPC to remove these surfaces. An euclidian clustering is applied to the rest of the cloud that geometrically separates it into sub-clouds. RANSAC is used again to check the validity of each sub-cloud, if the sub-cloud is composed mainly of planer surfaces then it is removed. Hence, the remaining of CPC contains only the set of candidates to be used as input for classifier.

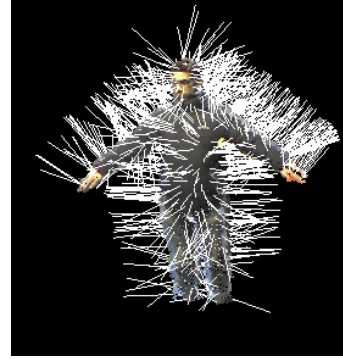


Figure 3: Example of surface normals shown at randomly chosen points from a CPC.

2.2 Descriptor Construction

The proposed 3D descriptor transposes the HOG into 3D point clouds. In HOG a window is densely subdivided into a uniform grid of blocks. In each block the gradient orientations over the pixels are computed and collected in a 1D histogram. In the 3D point cloud the gradient is meaningless. So it is replaced by the surface normal at each point (Figure 3). The local surface normal is estimated for each point p using the least-mean square plane fitting (Holz et al., 2012). The method works by fitting a plane to the set of neighbouring points of p , and the normal of the plane is assigned to point p . The point clouds acquired by the kinect could contain some artifacts and noise. This does not affect the surface normal estimation process as the used method can provide good results even with the presence of noise.

The 3D space is divided into sub-areas (blocks). We use a cylindrical subdivision similar to the one proposed by Gond (Gond et al., 2008) for his work on pose recognition from voxel reconstruction. Hence we respect the axial symmetry of the human class. The point cloud is included inside a cylinder perpendicular with the ground plane and divided as follows:

- First a radial cut divides the cylinder (Figure 4a).
- Second an azimuth cut divides the cylinder into sectors (Figure 4b).
- Third an axial cut across the cylinder main axis subdivides the cylinder into sections (Figure 4c).

The resulting block is a shell sector as represented in (Figure 4d). Figure 5 shows an illustration of this process over a point cloud. Each block contains a certain number of 3D points and then the histogram of oriented normal is computed.

Since a normal is a 3D vector it can not be associated to a 1D histogram. To solve this problem we used the generic 3D orientation quantization proposed by

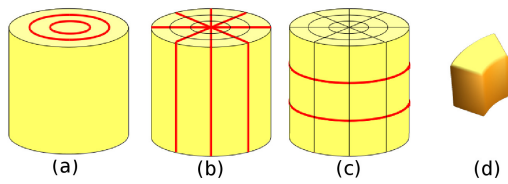


Figure 4: Cylindric subdivision into blocks: a radial cut (a), an azimuth cut (b) and an axial cut (c). The resulting block (d).

Kläser (Kläser et al., 2008).

The normal vector is placed inside a regular polyhedron (Figure 6) and then projected onto the faces of the polyhedron. Each face of the polyhedron corresponds to a bin of the histogram. The projection of the normal vector on a face is computed by:

$$p(\vec{n}, f) = \begin{cases} \vec{n} \cdot \vec{n}_f, & \text{if } \vec{n} \cdot \vec{n}_f > 0 \\ 0 & \text{otherwise} \end{cases} \quad (5)$$

where \vec{n} is the normal vector and \vec{n}_f is the vector from the center of the polyhedron to the center of the face f (Figure 7).

Then the histogram related to the block b is computed by:

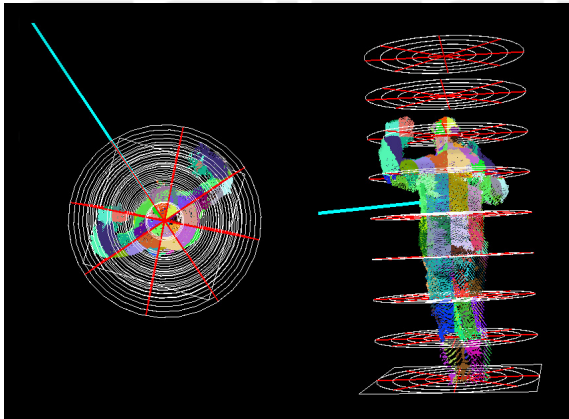


Figure 5: Dividing a candidate into blocks, where each block is represented by a different color.

$$H_b(f) = \frac{h_b(f)}{\sum_{f'} h_b(f')} \quad (6)$$

$$h_b(f) = \sum_{\vec{n} \in C_b} p(\vec{n}, f) \quad (7)$$

where C_b is the set of normal vectors on points inside of block b .

The concatenation of all the histograms provides the descriptor.

$$D = H_1 \cdot H_2 \cdot \dots \cdot H_{N_b} \quad (8)$$

where N_b is the number of blocks.

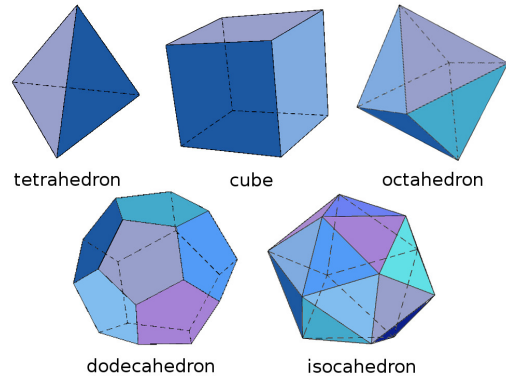


Figure 6: The five regular polyhedrons.

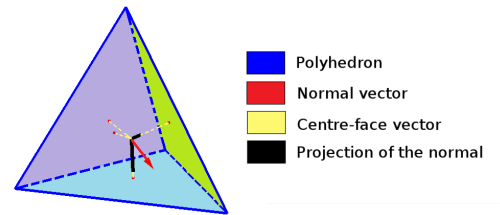


Figure 7: Projection of normal vector for 3D orientation quantization.

2.3 Classification

As mentioned previously, the proposed method works on a complete 3D point cloud which is acquired in an indoor environment. To our knowledge, there is no training database that provides such types of data. For this purpose we have decided to build an original database of CPCs. The database comprises two types of examples: positives (Human) and negatives (random objects that can be found in an indoor environment) (Figure 8). The positive part of the database dedicated to human subjects contains 600 point clouds. This part was constructed from 17 different persons with various poses, shapes and clothing. The negative part of the database contains the non-human examples, and it consists of approximately 600 point clouds. It contains elements that could appear in an indoor scene: furniture, stacks of cartons, computer equipment, etc. Objects that has similar dimension to human body shape (for example clothes rack where we are put clothes) are formed to make challenging experimental tests. When constructing the database, only one subject is placed in the middle of the scene. The frontal direction information of each human subject is saved while performing different positions. The information about the direction will be used in the learning step and also in the testing step as a ground truth.

A Support Vector Machine (SVM) classifier (Chang and Lin, 2011) was chosen to train a classification



Figure 8: Examples of CPC of human (left) and non-human subjects (right).

model. The SVM uses for this task the descriptors calculated from the set of positive and negative examples. The classification model will also allow the determination of the frontal orientation of the person. This is achieved with the help of the information about the frontal direction vector of each positive example in the database. When testing a human candidate we choose an arbitrary direction vector and then rotate it several times. Hence, each rotation of the direction vector will result in a different descriptor. These descriptors are tested by the classification model and the descriptor with the highest positive score provides the orientation of the human.

3 EXPERIMENTS

In this section we present the evaluation of our classification method. The first round of experiments was conducted to assess the efficiency of our descriptor. We show the results of testing our method on data set of positives and negatives CPC examples. In the second set of experiments, we performed two types of comparisons. First, we compare the results of CPC with those obtained by using single point clouds. Different scenarios are presented. In the second comparison stage, we performed a comparison between the proposed 3D descriptor and the one introduced in (Munaro et al., 2012). Finally, the last experiments were conducted experiments in order to validate the orientation estimation.

3.1 Efficiency

Since there is no similar database in the literature we created two sets of examples to evaluate the classification and to optimize the different required parameters of the method. Each set contains 64 positive and 64 negative examples. The two sets were acquired using our multi-kinect platform similarly to the training data. The examples in each set were then tested by the classification model. The trained classification model returns a score that corresponds to the probability that the point cloud is a human. The first set was more challenging and the results obtained from this set are presented in the following sections. The second set provides absolutely perfect results.

There are several parameters used to compute the 3D descriptor (Table 1). We repeat the classification test several times with different combinations of descriptor parameters. Figure 9 and Figure 10 show the results obtained from different values for the cylinder radius and polyhedron parameters respectively. Table 1 shows the best value for each parameter. With the best configuration of parameters, we obtain a precision of 0.97 and a recall of 0.97, which gives a $F_{measure}$ of 0.97. These excellent results validate the efficiency of our method.

A descriptor is computed in about 30ms with a non-optimized C++ implementation running on a 3GHz processor. With further optimization the descriptor can be used in applications that require real-time performance such as patient surveillance and gait assessment.

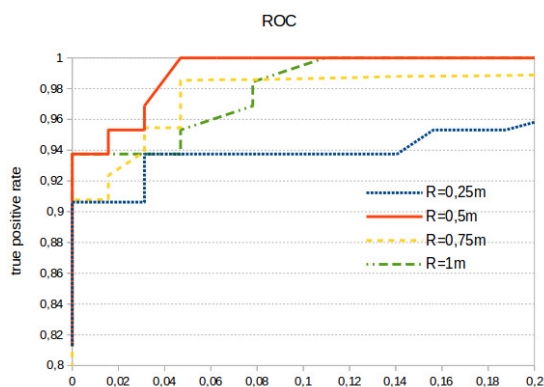


Figure 9: ROC curves obtained with different values of cylinder radius.

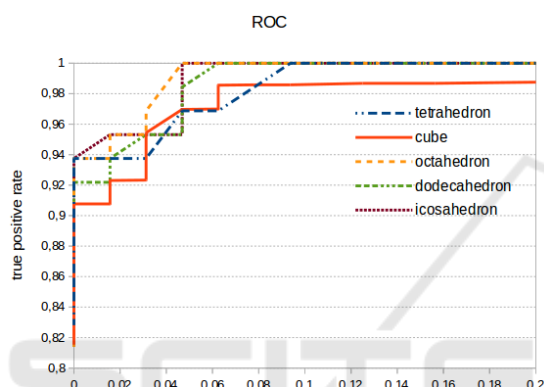


Figure 10: ROC curves obtained with different types of polyhedrons.

Table 1: Descriptor parameters.

| Parameter | Value |
|----------------------|------------|
| Cylinder Height | 2 meter |
| Cylinder Radius | 0.5 meter |
| Polyhedron | octahedron |
| Cylinder Radial Cut | 5 circles |
| Cylinder Azimuth Cut | 8 sectors |
| Cylinder Axial Cut | 8 sections |

3.2 Complete vs Single Point Cloud

To illustrate the benefits of using a CPC from a multi-kinect system we repeat the process of classification in two different scenarios. In the first scenario we assume that the kinects are working independently and we compute the descriptors from the Single Point Cloud (SPC) that come from each kinect separately. In the second scenario we consider that the kinects are working together but the output of this multi-kinect system is a set of SPCs, and of course the number of these SPCs is equivalent to number of the kinects in the system. In this scenario we take only the SPC with the maximum classification result (Max-SPC).

Figure 11 shows the ROC curves for the three experiments. We notice that using a single camera significantly decreases the classification performances. This shows the advantages of using multi-kinect platform over single sensors approaches. On the other hand, the CPC curve is above the Max-SPC one which also confirms that working with a CPC is better than using separated point clouds independently.

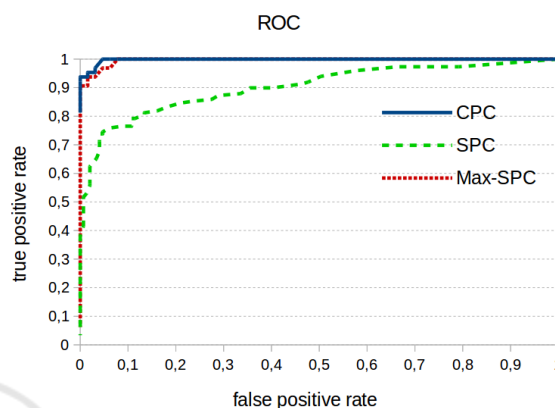


Figure 11: ROC curves obtained from our complete point cloud (CPC) and with the point cloud of each kinect taken individually (SPC) or combined (Max-SPC). A single view decreases significantly the performances and our CPC outperforms the combination of single point cloud.

3.3 Comparison with HOG

We have compared our method with HOG descriptor for 3D camera developed in (Munaro et al., 2012). The method works by selecting a set of candidate clusters from the point clouds and then apply HOG classification method on the corresponding 2D color image of these clusters. For comparison we used a dataset of 80 complex scenes. Each scene represents an indoor location with different objects and only one person. There are five different persons in this data set, each of them performing various poses. For each scene we obtained the CPC and also the separate single point clouds from each kinect. We applied our method on the CPC and the method of (Munaro et al., 2012) is applied separately on each of the other single point clouds. The obtained results are shown on Table 2. HOG-SC (Single Image) corresponds to the classification result of (Munaro et al., 2012) from a single kinect. In HOG-CC (Combined Camera) a cluster provides a detection if it was detected from at least one kinect with (Munaro et al., 2012). Once again, a single point of view provides low performances. Our method outperforms the combination of (Munaro et al., 2012) processed on the three kinects especially with the recall criterion.

Table 2: Classification performances of our method compared with HOG applied on a single color image (HOG-SC) then applied on the color images acquired by the all cameras (a person is detected if he is detected at least in one of the color image) (HOG-CC). We notice that our method provides the best results.

| Method | Precision | Recall | $F_{measure}$ |
|------------|-------------|-------------|---------------|
| our method | 0.99 | 0.86 | 0.92 |
| HOG-SC | 0.93 | 0.22 | 0.36 |
| HOG-CC | 0.91 | 0.51 | 0.66 |

In Figure 12 some examples where HOG process is failed are shown while our descriptor shows very good robustness.

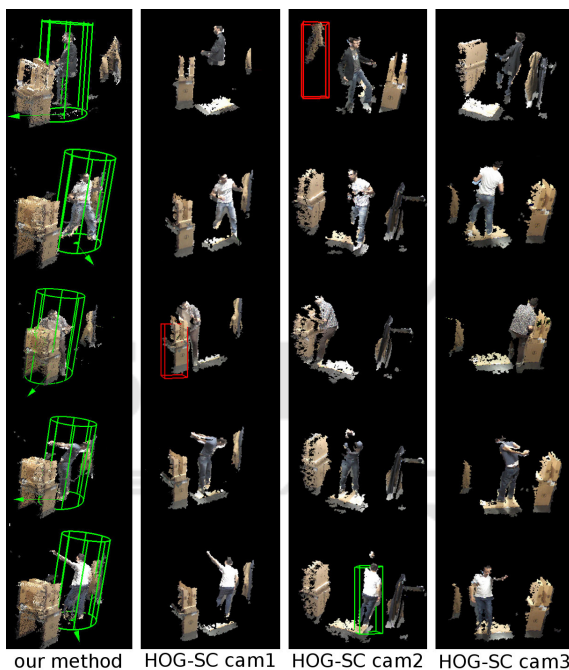


Figure 12: Examples of scenes where a simple HOG process is failed and our method succeeds. Green lines correspond to true detections and red lines correspond to false detections.

3.4 Orientation Estimation

In order to evaluate the orientation estimation, we tested for each positive example several hypothetical frontal orientations. We choose an arbitrary direction and rotate it around the subject's vertical axis. In our case we performed the rotation 4 times (i.e we increase the rotation angle by 90°), and at each rotation we computed the descriptor using the corresponding orientation vector. For each positive example from the test dataset, we compared the orientation of descriptor with the highest score with the ground-truth orientation. The orientation was correctly estimated

for a vast majority of examples in the dataset (90%), except for some situations (8%) where the back is estimated as the frontal orientation resulting in a 180° error. This is due to the fact that when a person's arms are parallel to its torso, the 3D surface of the front and back views are very similar. The orientation for the remaining 2% were estimated with 90° error from the ground truth.

4 CONCLUSIONS

In this paper we proposed a new 3D descriptor for the human classification which estimates the orientation of the human. The proposed descriptor uses complete 3D point clouds provided by a multi-kinect system. To validate it, we built an original database. The classification performs with an excellent precision. Two main contributions can be highlighted: first the use of the surface normal orientation and cylindrical space division to compute a human descriptor and second the set-up of a multi-kinect platform to acquire complete point cloud. We have proved that this acquisition framework improves significantly the detection performance.

In this paper, we focused on the classification of isolated subjects. Future work includes the complete detection process by a dense scan of the scene. For this purpose, we will work with scenarios where several persons are present in the scene. The cylinder will scan across the scene at all positions and conventional non-maximum suppression will be run on the output to detect human instances.

ACKNOWLEDGEMENTS

The authors gratefully acknowledge the support of Région de Bourgogne for this work.

REFERENCES

- Chang, C. C. and Lin, C. J. (2011). Random sample consensus: A paradigm for model fitting with applications to image analysis and automated cartography. *Transactions on Intelligent Systems and Technology*, 27:1–27.
- Choi, B., Mericli, C., Biswas, J., and Veloso, M. (2013). Fast human detection for indoor mobile robots using depth images. *International Conference on Robotics and Automation*, pages 1108–1113.
- Choi, B., Pantofaru, C., and Savarese, S. (2011). Detecting and tracking people using an rgb-d camera via multiple detector fusion. *Conference on Computer Vision Workshops*, pages 6–13.

- Dalal, N. and Triggs, B. (2005). Histograms of oriented gradients for human detection. *Computer Vision and Pattern Recognition*, 1:886–893.
- Deveaux, J. C., Hadj-Abdelkader, H., and Colle, E. (2013). A multi-sensor calibration toolbox for kinect : Application to kinect and laser range finder fusion. *International Conference on Advanced Robotics*.
- Essmaeel, K., Gallo, L., Damiani, E., De Pietro, G., and Dipanda, A. (2012). Multiple structured light-based depth sensors for human motion analysis: A review. *Ambient Assisted Living and Home Care*, 7657:240–247.
- Fischler, M. A. and Bolles, R. C. (1981). Random sample consensus: A paradigm for model fitting with applications to image analysis and automated cartography. *Commun. ACM*, 24:381–395.
- Gond, L., Sayd, P., Chateau, T., and Dhome, M. (2008). A 3d shape descriptor for human pose recovery. *Lecture Notes in Computer Science*, 5098:370–379.
- Holz, D., Holzer, S., Rusu, R. B., and Benke, S. (2012). Real-time plane segmentation using rgb-d cameras. *Lecture Notes in Computer Science*, pages 306–317.
- Ikemura, S. and Fujiyoshi, H. (2011). Real-time human detection using relational depth similarity features. *Asian Conference on Computer Vision*, pages 25–38.
- Klaser, A., Marszalek, M., and Schmid, C. (2008). A spatio-temporal descriptor based on 3d-gradients. *British Machine Vision Conference*, pages 275:1–10.
- Munaro, M., Basso, F., and Menegatti, E. (2012). Tracking people within groups with rgb-d data. *International Conference on Intelligent Robots and Systems*, pages 2101–2107.
- Raposo, C., Barreto, J. P., and Nunes, U. (2013). Fast and accurate calibration of a kinect sensor. *International Conference on 3D Vision*, pages 342–349.
- Song, S. and Xiao, J. (2014). Sliding shapes for 3d object detection in depth images. *European Conference on Computer Vision*.
- Spinello, L. and Arras, K. O. (2011). People detection in rgb-d data. pages 3838–3843.
- Tang, S., Wang, X., Lv, X., Han, T. X., Keller, J., He, Z., Skubic, M., and Lao, S. (2012). Histogram of oriented normal vectors for object recognition with a depth sensor. *Asian Conference on Computer Vision*, 7725:525–538.
- Tian, Q., Zhou, B., Zhao, W., Wei, Y., and Fei, W. (2013). Human detection using hog features of head and shoulder based on depth map. *Journal of Software*, 8:2223–2230.
- Xia, L., Chen, C., and Aggarwal, J. K. (2011). Human detection using depth information by kinect. *Computer Vision and Pattern Recognition Workshops*, pages 15–22.